Relaxation and Dephasing in a Two-Electron 13C Nanotube Double Quantum Dot

Churchill, H O H; Kuemmeth, Ferdinand; Harlow, J W; Bestwick, A J; Rashba, E I; Flensberg, K; Stwertka, C H; Taychatanapat, T; Watson, S K; Marcus, C M

Published in:
Physical Review Letters

DOI:
10.1103/PhysRevLett.102.166802

Publication date:
2009

Document version
Publisher's PDF, also known as Version of record

Relaxation and Dephasing in a Two-Electron ^{13}C Nanotube Double Quantum Dot

H. O. H. Churchill,[1] F. Kuemmeth,[1] J. W. Harlow,[1] A. J. Bestwick,[1] E. I. Rashba,[1,2] K. Flensberg,[3] C. H. Stwertka,[1] T. Taychatanapat,[1] S. K. Watson,[1,*] and C. M. Marcus[1,†]

[1]Department of Physics, Harvard University, Cambridge, Massachusetts 02138, USA
[2]Center for Nanoscale Systems, Harvard University, Cambridge, Massachusetts 02138, USA
[3]Nano-Science Center, Niels Bohr Institute, University of Copenhagen, Universitetsparken 5, DK-2100 Copenhagen, Denmark

(Received 19 November 2008; published 22 April 2009)

We use charge sensing of Pauli blockade (including spin and isospin) in a two-electron ^{13}C nanotube double quantum dot to measure relaxation and dephasing times. The relaxation time T_1 first decreases with a parallel magnetic field and then goes through a minimum in a field of 1.4 T. We attribute both results to the spin-orbit-modified electronic spectrum of carbon nanotubes, which at high field enhances relaxation due to bending-mode phonons. The inhomogeneous dephasing time T_2^* is consistent with previous data on hyperfine coupling strength in ^{13}C nanotubes.

DOI: 10.1103/PhysRevLett.102.166802 PACS numbers: 73.22.Dj, 71.70.Ej, 71.70.Jp, 73.63.Fg

Few-electron double quantum dots have enabled the coherent manipulation and detection of individual and coupled electron spin states required to form qubits [1–4]. Although recent protocols mitigate decoherence due to hyperfine coupling in GaAs-based devices [5,6], an attractive alternative is to base spin qubits on group IV elements, which primarily comprise isotopes free of nuclear spins. Progress in this direction includes double quantum dots in Si/SiGe two-dimensional electron gases [7], P donors in Si [8], Ge/Si nanowires [9], and carbon nanotubes [10]. Recent advances in nanotube double dots include observation of singlet-triplet physics [11] and Pauli blockade [12]. Developing these systems as spin qubits depends crucially on understanding their modes of relaxation and dephasing.

This Letter reports measurements of relaxation and dephasing times in a two-electron nanotube double quantum dot grown from isotopically enriched (99%) ^{13}C methane. Measurements use fast pulses applied to electrostatic gates combined with charge-sensing measurements in the Pauli-blockade regime, including spin and isospin quantum states. The relaxation time of these states T_1 initially decreases with parallel field and has a minimum in a field of 1.4 T. We interpret these results within the context of the recently observed [13] spin-orbit interaction in carbon nanotubes [14,15]. We also measure a relatively short two-electron inhomogeneous dephasing time $T_2^* \sim 3$ ns, which presumably arises from hyperfine coupling. The implied hyperfine coupling strength is consistent with values measured recently by transport [16]. In contrast, the longer $T_1 \sim 1$ μs does not show signatures of hyperfine coupling.

The double dot studied here is based on a single-walled carbon nanotube grown by chemical vapor deposition using 99% $^{13}CH_4$ feedstock [17,18]. After deposition of two pairs of Pd contacts [Fig. 1(a), red], the device is coated with a 30 nm functionalized Al_2O_3 top-gate oxide using atomic layer deposition [19,20]. Aluminum top gates (blue, yellow, and gray) define a double dot between contacts 1 and 2 and a single dot between contacts 3 and 4, capacitively coupled [orange wire in Fig. 1(a)] to the double dot to allow charge sensing [9,21]. The small band gap (~25 meV) nanotube is operated in the electron regime. Direct current and standard lock-in measurements are carried out in a dilution refrigerator (electron temperature ~100 mK).

Electron occupancies (N_L, N_R) of the double dot are determined from the charge stability diagram [Fig. 1(b)],

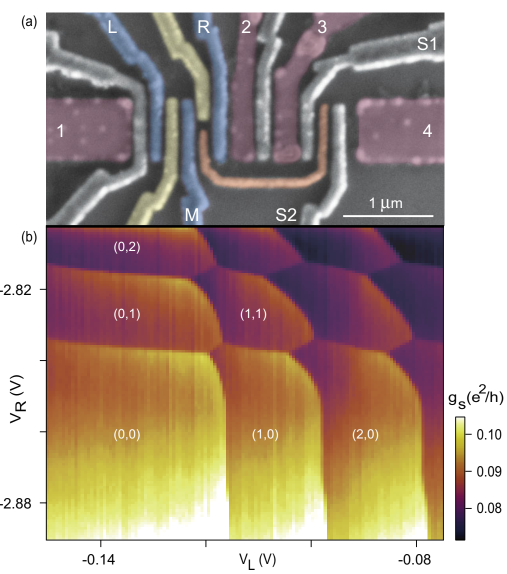

FIG. 1 (color online). (a) False-color scanning electron micrograph of a device of the same design as the measured device. The ^{13}C nanotube (not visible) runs horizontally under Pd contacts (red). The double dot is defined by top gates L, R, and M (blue). On the same nanotube, a separate quantum dot is controlled with gates $S1$ and $S2$ and capacitively coupled (orange wire) to the double dot to allow charge sensing. Fast pulses are applied to L and R. (b) Charge sensor conductance g_s measured between contacts 3 and 4 as a function of V_L and V_R showing the charge stability diagram, with electron occupancies (N_L, N_R) in each dot.

measured using the conductance g_s of the charge-sensing dot [9]. Lever-arm ratios converting gate voltages to dot energies, extracted from nonlinear transport, give a large (~1 meV) interdot capacitive coupling, based on the size and shape of the stability diagram.

Single-electron states of a nanotube quantum dot (in the lowest circumferential mode) can be classified by a quantized longitudinal mode, a real spin ($S = 1/2$), and an isospin, reflecting two valleys K and K' (or, equivalently, clockwise and counterclockwise motion around the nanotube circumference) [22]. Including both spin and isospin, there are 16 ways to fill the lowest longitudinal modes with two electrons in the separated (1, 1) charge state. There are only six ways, however, to fill the lowest longitudinal mode of (0, 2) while maintaining overall antisymmetry of the two-electron wave function.

Under the condition of conserved spin and isospin in the double dot [23], the remaining 10 of the 16 two-electron states of (1, 1) may be blocked from tunneling to the lowest mode of (0, 2) by selection rules on both spin and isospin. This is a generalization of the Pauli blockade [24] observed in few-electron double dots without valley degeneracy. Previous experiments on Pauli blockade have considered only spin selection rules.

Pauli blockade of the $(1, 1) \rightarrow (0, 2)$ transition is detected by time-averaged charge sensing, using the cyclic gate-pulse sequence in Fig. 2(b) [25]: Starting at E in (0, 1), an electron is loaded with random spin and isospin, forming a (1, 1) state at point R. Moving to point M (adiabatically on the time scale of interdot tunnel coupling) where the ground state is (0, 2) and remaining there for a time τ_M, the system may or may not tunnel to (0, 2) depending on the state of (1, 1). Blocked states would have to tunnel to states involving higher-lying longitudinal modes of (0, 2), which are energetically inaccessible at M (they are $\gtrsim$1 meV higher [16]); such states must flip either real spin or isospin (or both) to reach an accessible (0, 2) state.

With the cycle $E \rightarrow R \rightarrow M \rightarrow E$ running continuously, V_L and V_R are rastered in the vicinity of the (1, 1)-(0, 2) charge transition [Fig. 2(b)]. Eighty percent of the pulse period is spent at M (10% each for E and R) so that the time-averaged sensor signal g_s primarily reflects the charge state at M. Within the triangle marked by solid white lines in Figs. 2(c) and 2(d), the time-averaged g_s lies between values on the (1, 1) and (0, 2) plateaus, decreasing in visibility as τ_M is increased [Fig. 2(c)], with edges of the triangle disappearing faster due to thermal activation [25]. We also observe faster relaxation within 200 μeV of the base. On the contrary, g_s is independent of the pulse period outside the pulse triangle. A control cycle with R and M interchanged does not show a triangular region in (1, 1), indicating that none of the loaded (0, 2) states are blocked from tunneling into (1, 1) [Fig. 2(d)].

In a magnetic field B, applied within a few degrees of parallel to the tube axis, forward bias ($V_2 > V_1$) current—the Pauli-blockade direction—shows a dip around $B = 0$ [Fig. 3(a)], indicating a reduced spin- and/or isospin-flip

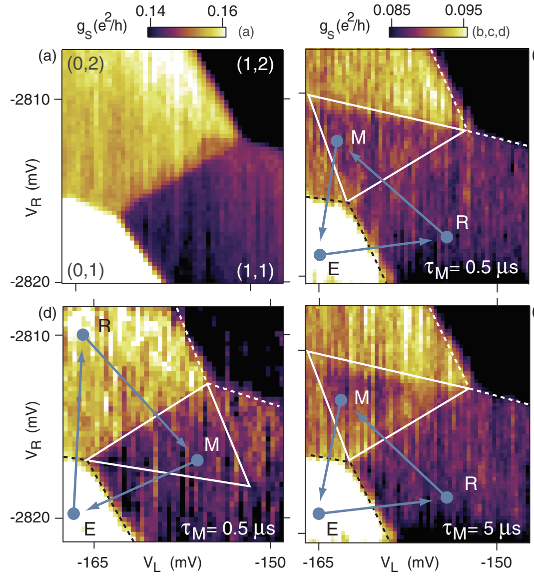

FIG. 2 (color online). Sensor conductance g_s as a function of V_R and V_L around the (1, 1)-(0, 2) transition (a) without applied pulses and (b) with the T_1 pulse cycle $E \rightarrow R \rightarrow M \rightarrow E$ applied, $\tau_M = 0.5$ μs $< T_1$. Dashed lines indicate the boundaries of (0, 1) and (1, 2) during step M. Within the pulse triangle (solid white lines), g_s is between the (1, 1) and (0, 2) values, indicating partially blocked tunneling from (1, 1) to (0, 2), (c) with the T_1 pulse cycle, $\tau_M = 5$ μs $> T_1$, and (d) the control pulse cycle, with R and M interchanged. $B = 0$ in each panel. Blue arrows are schematic: Point E is farther left than shown so that the pulse cycle encloses the (0, 1)-(1, 1)-(0, 2) vertex for all points M within the pulse triangle.

rate near zero field. A phenomenological Lorentzian fit (red curve) to the dip has a FWHM of 11 mT. In the reverse-bias case ($V_1 > V_2$), current is independent of B (~1 pA) over the same range.

The pulse-triangle visibility $I = \frac{g_s(\tau_M) - g_s(\infty)}{g_s(0) - g_s(\infty)}$ as a function of τ_M, measured in the center of the triangle [Figs. 2(b) and 2(c)] at $B = 0$, 100, and 200 mT, is shown in Fig. 3(b) along with the relaxation time T_1 extracted from fits to $I(\tau_M) = \frac{1}{\tau_M}\int_0^{\tau_M} e^{-t/T_1} dt$ [25]. The relaxation time decreases with increasing B but with a weaker dependence than the transport data [Fig. 3(a)]. We speculate that these trends are due to phonon-mediated relaxation enabled by spin-orbit coupling [13,15,26], a mechanism that is suppressed at small magnetic fields by Van Vleck cancellation [27].

Characteristics of the single-particle spectrum of the individual dots can be inferred from the B dependence of the addition spectrum, measured for the left dot via charge sensing [Fig. 3(c)]. Field dependences of the addition energies for the first four electrons suggest the spectrum shown in Fig. 3(d), consistent with Ref. [13] [28], with spin-orbit coupling playing an important role. We note, in particular, that the energy to add the second electron first increases with B at small B and then decreases at higher field. This indicates that the second electron first occupies a

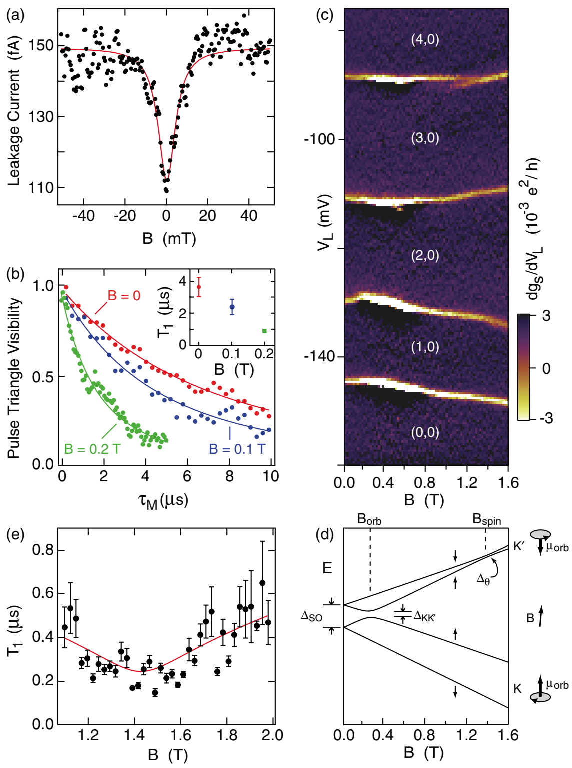

FIG. 3 (color online). (a) Leakage current through blockade near zero detuning for small B, $V_{12} = -2$ mV. (b) Decay of pulse-triangle visibility I as a function of τ_M measured in the center of the triangle at several values of B. (c) dg_s/dV_L as a function of V_L and B, showing the dependence of ground state energies on B for the first four electrons on the left dot. (d) Energy level diagram of the lowest states of a nanotube with spin-orbit coupling; $\Delta_{SO} = 170$ μeV, $\Delta_{KK'} = 25$ μeV, $\theta = 5°$, and $\mu_{orb} = 330$ μeV/T. Arrows indicate the spin component parallel to the nanotube axis. Schematics (right) indicate orbital magnetic moment μ_{orb} for clockwise (K) and counterclockwise (K') moving isospin states. At B_{orb} (B_{spin}), the orbital (Zeeman) shifts compensate Δ_{SO} and states with opposite isospin (spin) anticross. (e) T_1 extracted as in (b) for B between 1.1 and 2 T. Error bars: Standard deviation of the fit parameter T_1. One-parameter fit (red curve) to theory of Ref. [15], modified for B misaligned by 5° (see text).

counterclockwise (K') isospin state at small B and then changes to a clockwise (K) isospin at $B \sim 250$ mT. The energy to add the third electron does the opposite. Fits to the low field slopes for the second and third electron addition energies yield moments of 390 and -270 μeV/T, respectively, with a difference in magnitudes within 10% of $2\mu_B$, a signature of a spin-orbit-dominated spectrum [13]. Thus we infer an orbital moment $\mu_{orb} = 330$ μeV/T and a zero-field spin-orbit splitting $\Delta_{SO} = 170$ μeV.

A consequence of the spectrum in Fig. 3(d) is a predicted [15] minimum in T_1 as the two K' states with opposite spin approach one another at $B_{spin} = \Delta_{SO}/g\mu_B$, which for this nanotube occurs at 1.4 T [cf. Fig. 3(d)]. The expected coupling of these two states is via 1D bending-mode phonons with quadratic dispersion, leading to a $T_1 \propto \sqrt{\Delta}$ dependence on the energy splitting Δ due to the density-of-states singularity at zero energy in 1D [15]. This is in contrast to higher dimensions, where T_1 diverges as $\Delta \rightarrow 0$ [15,27,29].

Values for T_1, extracted from fits as in Fig. 3(b), are shown in Fig. 3(e), where a minimum in T_1 is observed at the predicted value $B \sim 1.4$ T. Also shown in Fig. 3(e) is a fit of the form $T_1 = C\sqrt{\Delta_\theta}$, where the splitting $\Delta_\theta = g\mu_B\sqrt{(B\cos\theta - \Delta_{SO}/g\mu_B)^2 + (B\sin\theta)^2}$ is anticrossed, accounting for a misalignment angle θ between the nanotube axis and the direction of the applied field [30]. For these fits, we use $g = 2$ and the measured quantities Δ_{SO} and θ (5° determined by the electron micrograph); the only free parameter is an overall scale for T_1, $C = 65$ ns$/\sqrt{\mu\text{eV}}$, only a factor of $\sim$5 smaller than the estimates in Ref. [15]. Attributing the measured T_1 minimum to this mechanism requires loading a two-electron state involving at least one of the two higher states of Fig. 3(d) at step R, which is expected because the levels of the left dot are well below the electrochemical potential of the left lead at R. We note that hyperfine relaxation should also be strongest near a degeneracy [25], but the ratio $\Delta_\theta/(g\mu_B B_{nuc}) \sim 20$ (Ref. [16]) would require huge inelastic tunnel rates ruled out by transport measurements to explain the measured T_1.

We do not observe signatures of hyperfine-mediated relaxation near $B = 0$ [31], but note that a difference in effective magnetic fields between the two dots should induce dephasing of prepared two-particle spin and isospin states. To measure the inhomogeneous dephasing time T_2^* of a state at $B = 0$, a pulse cycle [Fig. 4(a)] first prepares an $(0, 2)$ state at P, then separates the electrons via P' into $(1, 1)$ at S for a time τ_s, and finally measures the return probability to $(0, 2)$ at M [3]. For small τ_s, the prepared state always returns to $(0, 2)$. For $\tau_s \gtrsim T_2^*$, a fraction of prepared states evolves into blocked states, reducing the return probability within the pulse triangle [Fig. 4(a)].

The dephasing time is obtained from the value of g_s in the center of the pulse triangle versus τ_s, which reflects the probability of return to $(0, 2)$ when calibrated against the equilibrium $(1, 1)$ and $(0, 2)$ values of g_s [Fig. 4(b)]. A likely source of dephasing is the hyperfine interaction. Assuming a difference in Overhauser fields acting on the two electrons of root mean square strength $\delta B_{nuc}^{||}$ parallel to the nanotube axis [5,32], the decay is fit to a Gaussian form, giving $T_2^* = \hbar/g\mu_B\delta B_{nuc}^{||} = 3.2$ ns. The corresponding $\delta B_{nuc}^{||} = 1.8$ mT is a factor of 2 smaller than our estimate of the single dot nuclear field B_{nuc} in ^{13}C nanotubes [33]. The difference may be due to anisotropic dipolar hyperfine coupling [34] or to accidental suppression of $\delta B_{nuc}^{||}$ [5]. Future work on ^{12}C nanotubes will allow dephasing mechanisms other than the hyperfine interaction to be investigated.

Finally, we note that the saturation value of the return probability in Fig. 4(c) is 0.17, smaller than the value of

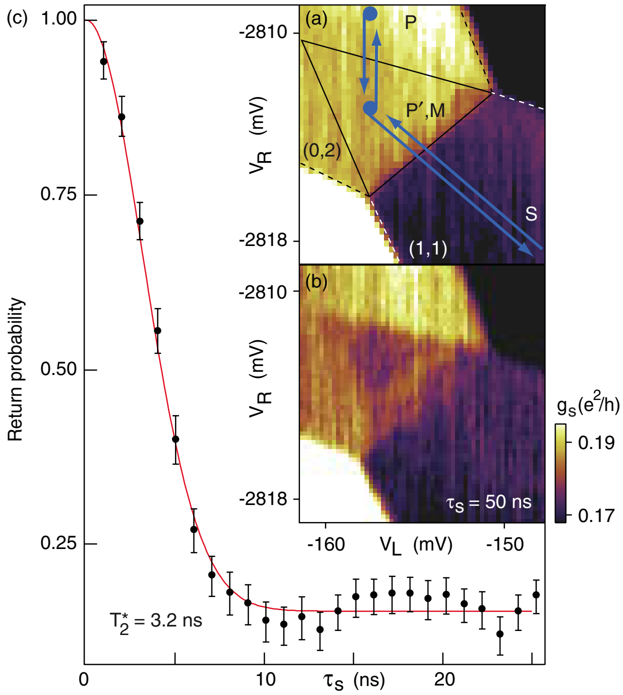

FIG. 4 (color online). (a) Pulse sequence to measure the dephasing time T_2^* (see text). If a state prepared at P dephases into a Pauli-blocked state while separated at S for a time τ_s, g_s is reduced within the pulse triangle outlined in black [shown in (b) for $\tau_P = \tau_{P'} = 100$ ns, $\tau_S = 50$ ns, and $\tau_M = 2\ \mu$s at $B = 0$]. (c) g_s calibrated to reflect the return probability to (0, 2) versus τ_s. A Gaussian fit (red) [32] gives $T_2^* = 3.2$ ns and $\delta B_{\rm nuc}^{||} = 1.8$ mT. The data points are an average of 500 individual traces; error bars are the standard error.

1/3 for singlet-triplet dephasing at $B = 0$ in GaAs [3,35], likely due to the richer spectrum allowed by isospin. Similarly, the tunneling probability from (1, 1) to (0, 2) [inferred from the visibility of the T_1 pulse triangle for $\tau_M = 0.5\ \mu s < T_1$, Fig. 2(b)] is ~0.15, lower than the 0.375 expected from state-counting arguments (6 unblocked states out of 16 total) combined with adiabatic passage. This issue requires further study.

In summary, we have measured relaxation and dephasing in a two-electron ^{13}C nanotube double quantum dot. We identify signatures of spin-orbit coupling in the magnetic field dependence of both the addition spectrum and the relaxation time T_1, and we observed a dephasing time T_2^* consistent with recent measurements of the hyperfine coupling strength in ^{13}C nanotubes. The short dephasing time motivates development of nanotube devices with less than the 1% natural abundance of ^{13}C.

We thank C. Barthel, E. A. Laird, and D. J. Reilly for technical assistance. This work was supported by the National Science Foundation under Grant No. NIRT 0210736, ARO/iARPA, the Department of Defense, and Harvard's Center for Nanoscale Systems. H. O. H. C. acknowledges support from the NSF.

*Present address: Department of Physics, Middlebury College, Middlebury, VT 05753, USA.
†marcus@harvard.edu

[1] D. Loss and D. P. DiVincenzo, Phys. Rev. A **57**, 120 (1998).
[2] R. Hanson *et al.*, Rev. Mod. Phys. **79**, 1217 (2007).
[3] J. R. Petta *et al.*, Science **309**, 2180 (2005).
[4] F. H. L. Koppens *et al.*, Nature (London) **442**, 766 (2006).
[5] D. J. Reilly *et al.*, Science **321**, 817 (2008).
[6] F. H. L. Koppens, K. C. Nowack, and L. M. K. Vandersypen, Phys. Rev. Lett. **100**, 236802 (2008).
[7] N. Shaji *et al.*, Nature Phys. **4**, 540 (2008).
[8] V. C. Chan *et al.*, J. Appl. Phys. **100**, 106104 (2006).
[9] Y. Hu *et al.*, Nature Nanotech. **2**, 622 (2007).
[10] N. Mason, M. J. Biercuk, and C. M. Marcus, Science **303**, 655 (2004).S. Sapmaz *et al.*, Nano Lett. **6**, 1350 (2006). M. R. Gräber *et al.*, Phys. Rev. B **74**, 075427 (2006).
[11] H. I. Jørgensen *et al.*, Nature Phys. **4**, 536 (2008).
[12] M. R. Buitelaar *et al.*, Phys. Rev. B **77**, 245439 (2008).
[13] F. Kuemmeth, S. Ilani, D. C. Ralph, and P. L. McEuen, Nature (London) **452**, 448 (2008).
[14] T. Ando, J. Phys. Soc. Jpn. **69**, 1757 (2000).
[15] D. V. Bulaev, B. Trauzettel, and D. Loss, Phys. Rev. B **77**, 235301 (2008).
[16] H. O. H. Churchill *et al.*, arXiv:0811.3236.
[17] L. Liu and S. Fan, J. Am. Chem. Soc. **123**, 11 502 (2001).
[18] $^{13}CH_4$ of 99% purity from Sigma-Aldrich. 2 nm diameter is estimated from atomic-force microscope measurements of similar growths.
[19] D. B. Farmer and R. G. Gordon, Nano Lett. **6**, 699 (2006).
[20] J. R. Williams, L. DiCarlo, and C. M. Marcus, Science **317**, 638 (2007).
[21] M. J. Biercuk *et al.*, Phys. Rev. B **73**, 201402(R) (2006).
[22] C. L. Kane and E. J. Mele, Phys. Rev. Lett. **78**, 1932 (1997).
[23] P. Jarillo-Herrero *et al.*, Nature (London) **434**, 484 (2005).
[24] K. Ono *et al.*, Science **297**, 1313 (2002).
[25] A. C. Johnson *et al.*, Nature (London) **435**, 925 (2005).
[26] Results in Ref. [16] required many-electron configurations where these spin-orbit effects are absent or diminished.
[27] A. V. Khaetskii and Yu. V. Nazarov, Phys. Rev. B **64**, 125316 (2001).
[28] Reference [15] infers the sign of the spin-orbit interaction from Ref. [14]. It is opposite to the sign found experimentally in Ref. [13] and here. As a result, the two lower, not upper, levels of our Fig. 3(d) cross in Ref. [15].
[29] S. Amasha *et al.*, Phys. Rev. Lett. **100**, 046803 (2008).
[30] This form is exact only for $\Delta_{KK'} = 0$ but is justified because orbital mixing is suppressed by large B.
[31] Hyperfine-mediated relaxation would reduce T_1 and increase leakage current near $B = 0$.
[32] J. M. Taylor *et al.*, Phys. Rev. B **76**, 035315 (2007).
[33] These data are for the device in [16] with $B_{\rm nuc} = 4$ mT.
[34] C. H. Pennington and V. A. Stenger, Rev. Mod. Phys. **68**, 855 (1996).
[35] D. J. Reilly *et al.*, Phys. Rev. Lett. **101**, 236803 (2008).